

RESEARCH ARTICLE

Changes in the Fine Composition of Global Forests from 2001 to 2020

Hongtao Xu¹, Bin He^{1,2*}, Lanlan Guo³, Xing Yan¹, Jinwei Dong⁴,
Wenping Yuan⁵, Xingming Hao⁶, Aifeng Lv⁷, Xiangqi He¹, and Tiewei Li²

¹State Key Laboratory of Earth Surface Processes and Resource Ecology, College of Global Change and Earth System Science, Geography Science Faculty, Beijing Normal University, Beijing 100875, China. ²Akesu National Station of Observation and Research for Oasis Agro-ecosystem, Akesu, Xinjiang Uygur Autonomous Region 843017, China. ³Geography Science Faculty, Beijing Normal University, Beijing 100875, China. ⁴Key Laboratory of Land Surface Pattern and Simulation, Institute of Geographic Sciences and Natural Resources Research, Chinese Academy of Sciences, Beijing 100101, China. ⁵Institute of Carbon Neutrality, Sino-French Institute for Earth System Science College of Urban and Environmental Sciences, Peking University, Beijing 100871, China. ⁶State Key Laboratory of Desert and Oasis Ecology, Xinjiang Institute of Ecology and Geography, Chinese Academy of Sciences, Urumqi, Xinjiang Uygur Autonomous Region 830011, China. ⁷Key Laboratory of Water Cycle and Related Land Surface Processes, Institute of Geographic Sciences and Natural Resources Research, Chinese Academy of Sciences, Beijing 100101, China.

*Address correspondence to: hebin@bnu.edu.cn

Knowledge of forest management types is key to sustainable forest restoration practices, forest biomass assessment, and carbon accounting. However, there are no available global forest-management maps because of the spectral similarity of different forest management types. As such, we applied random forest and change detection algorithms to generate annual maps of 6 forest management types at a spatial resolution of 250 m from 2001 to 2020 including naturally regenerated forest (unmanaged and managed), planted forest (rotation of >15 years and ≤15 years), oil palm plantation, and agroforestry. In general, validation results on a point scale show that the overall accuracy is 86.82% ± 9.14%, indicating that our annual maps accurately represent global spatiotemporal variations in forest management types. Furthermore, we estimated the annual biomass carbon stock of different forest management types. The net expanded areas of planted forest, oil palm plantation, and agroforestry offset 59.56% of the loss of forest area and 77.13% of the loss of biomass carbon stock due to the decrease in the naturally regenerated forest. The decrease of managed natural regeneration forests, the expansion of planted forests with a rotation period of more than 15 years, and agroforestry resulted from reforestation practices, while the expansion of planted forests with a rotation period of less than 15 years and oil palm plantations resulted from the removal of part of agroforestry. Moreover, the expansion of planted forests with a rotation of less than 15 years (72.73%) dominates the global expansion of planted forests, and China has contributed 42.20% of this expansion. Our results are beneficial for nature solution-based climate change mitigation.

Introduction

Forest ecosystems are the largest terrestrial ecosystems and absorb twice as much carbon as they emit each year [1], and thus have a critical role in climate change mitigation. Recently, studies of natural climate solutions (NCS) have revealed that forest practices (e.g., reforestation and natural forest management) have substantial potential for climate change mitigation [2–5]. This has made the science community, stakeholders, and governments more confident about ambitious programs such as voluntary zero deforestation and the Nature Forest Conservation Program in the Asia–Pacific region [6,7]. However, other studies have revealed that managed forest, especially planted forest, show too little carbon stock capacity to increase terrestrial carbon sink

and thereby mitigate global climate change because forest management practices affect the diversity and community composition of soil fungi [8–10]. Therefore, from a forest management perspective, the spatial pattern of global forests is important for addressing these issues.

Despite the availability of official statistical data that document the composition and trends of forest management types, spatiotemporal data are rarely reported. Attempts to generate global forest maps from a management perspective are limited to those with a small number of broad classes or a single period [11–13]. For example, Potapov et al. [12] generated the intact landscapes with a minimum area of 500 km² in 2000, 2013, and 2016 using a satellite-based mapping method based on a set of clear and straightforward criteria. However, this dataset

Citation: Xu H, He B, Guo L, Yan X, Dong J, Yuan W, Hao X, Lv A, He X, Li T. Changes in the Fine Composition of Global Forests from 2001 to 2020. *J. Remote Sens.* 2024;4:Article 0119. <https://doi.org/10.34133/remotesensing.0119>

Submitted 8 May 2023
Accepted 19 January 2024
Published 12 February 2024

Copyright © 2024 Hongtao Xu et al. Exclusive licensee Aerospace Information Research Institute, Chinese Academy of Sciences. Distributed under a Creative Commons Attribution License 4.0 (CC BY 4.0).

neglects the small intact forest patches. The United Nations Environment Programme World Conservation Monitoring Centre provided a natural and modified habitat layer (likely modified, potential modified, potential natural, and likely natural) at a spatial resolution of 1 km by the spatially overlapping anthropogenic pressure maps [14]; however, the source data used have their own uncertainty and definitions. Spatial Database of Planted Trees (SDPT V1.0) generated the global distribution of planted trees from national and local maps from various sources; however, there were inconsistent forest definitions of the collected maps and methods for planted tree mapping. Schulze et al. [13] generated 2 levels of forest management layers at a spatial resolution of 1 km in 2000 from forest planting (primary, secondary, and planted forest) and forest uses (production, multiple use, and other forest) perspectives based on a global allocation approach, while each level only consists of 3 forest categories. The absence of long-term global forest management maps is mainly due to the spectral similarities of different forest management types [15–17], which make it difficult to distinguish the various types. Specifically, spectral features vary globally with geography, tree species, and age classes for an individual forest management type. For a similar reason, spectral patterns also varied in other individual forest management types. This made a similar spectral pattern among different forest management types in certain bands or remote-sensing-derived indicators. The forest distribution and similarity of growth characteristics on a regional scale provide an alternative method for identifying different forest management types. Lesiv et al. [11] generated a map of the prevalent forest management layers (FML_v3, a version of the forest management layer) at a spatial resolution of 100 m. The layer displayed the distribution of different forest management types including intact forests, managed forests with natural regeneration, planted forests, plantation forest (rotation of <15 years), oil palm plantations, and agroforestry. However, the single period of FML_v3 provides insufficient information to investigate long-term variations in forest management types. The publicly available reference samples generated for FML_v3, and other available datasets, make it possible to generate long-term forest management maps at a spatial resolution of 250 m by combining variables indicative of the forest growth characteristics and regional distribution.

To provide global knowledge about the fine composition of forests and facilitate the decision making of sustainable forest restoration practices, forest biomass assessment, and carbon accounting, as well as provide scientific support to nature solution-based climate change mitigation, we carried out the global mapping of the fine composition of forests. Specifically, we generated the annual maps of the fine composition of forest from a forest management perspective at a spatial resolution of 250 m based on machine learning and change detection methods for the nominal years of 2001 to 2020 (Fig. S1). The forest management types were defined as naturally regenerating forests without signs of management (NRF-NM), naturally regenerating forests with signs of management (NRF-WM), planted forests with a rotation of >15 years ($PF_{>15}$), plantation forests with a rotation of ≤ 15 years ($PF_{\leq 15}$), oil palm plantations, and agroforestry [11]. Furthermore, we estimated the biomass carbon stocks in the different forest management types and investigated their temporal changes to understand the role of forest management types in climate mitigation.

Materials and Methods

Machine-learning-based forest management maps for 2001 to 2020

In this study, we generated the annual forest management maps for the nominal years of 2001 to 2020 at a spatial resolution of 250 m, based on random forest and change detection algorithms using multi-source datasets including MOD13Q1 imagery [18], human activity information extracted from the global terrestrial Human Footprint dataset [19], and terrain information extracted from the Global Multi-Resolution Terrain Elevation Data 2010 (GMTED2010, [20]). In this study, the 16-day observations of band reflectance values (B, R, NIR, and SWIR2) and vegetation indices at a spatial resolution of 250 m during 2001 to 2020 provided by MOD13Q1 imagery were aggregated into monthly scale using the maximum value composition method. The global terrestrial Human Footprint dataset provides an annual record of human activity at 1 km spatial resolution for 2000 to 2018, and the GMTED2010 provides the elevation information at a spatial resolution of 231.92 m. All datasets were applied to a unified Eckert 4 equal area projection at a resolution of 250 m.

To create the annual forest management maps, we first defined the study region by delineating the land cover categories of interest from 300 m ESA CCI land cover maps for 2001 to 2020 [21] and tree plantation extends from 3 other maps [11,13,22] (Supplementary Text 1 and Table S18). According to the forest categories described in Global Forest Resources Assessment [23], forests are composed of primary forests and planted forests. The primary forest includes naturally regenerated forests with no clearly visible indicators of human activities and with clearly visible indicators of human activities. In this study, based on the impact of human activities on natural regeneration forests, we classified the primary forests into naturally regenerating forests without management (NRF-NM) and naturally regenerating forests with management (NRF-WM). According to the forest management rotation cycles, planted forests can be reclassified as planted forests of short rotation and long rotation. The short rotation planted forests are characterized by dense rows of often one fast-growing species for timber production, such as eucalyptus, acacia, poplar, or willow, and are clear-cut after a maximum rotation period of 15 years due to the legal limitation to retain the high productivity of a young plantation [24]. In addition, 15 years is also a common choice as the maximum rotation period for short rotation planted forests in the previously published literature [25–27]. Therefore, in this study, based on a rotation cycle of 15 years, the planted forest was divided into the planted forest with a rotation of >15 years ($PF_{>15}$), and the planted forest with a rotation of ≤ 15 years ($PF_{\leq 15}$). In addition, we also considered other land use classes of trees such as oil palm plantation and agroforestry. Therefore, in this study, the forest was classified as naturally regenerating forest without management (NRF-NM), naturally regenerating forest with management (NRF-WM), planted forest with a rotation of >15 years ($PF_{>15}$), planted forest with a rotation of ≤ 15 years ($PF_{\leq 15}$), oil palm plantation, and agroforestry (Table S19). Given the similarity of the regional forest management composition due to the similar meteorological and soil conditions at the regional scale, such as tree species, and the increasing sensitivity of the random forest model to the training samples, the mapping was conducted separately for each continent.

To depict the differences between the forest management types, we calculated a total of 124 variables related to growth

characteristics and local textural information extracted from MOD13Q1 imagery, human activity information extracted from the global terrestrial Human Footprint dataset, and terrain information extracted from GMTED2010 (Table S20). In particular, variables related to growth characteristics were calculated at a monthly scale by considering the temporal changes using 5-year MOD13Q1 imagery before the nominal year. However, MOD13Q1 imagery used for the calculation of these variables is only available after 2000, and there was insufficient 5-year imagery to document the temporal changes for the nominal years prior to 2003. As such, we calculated these variables for 2001 to 2003 by considering the temporal changes using 5-year imagery after the nominal year. To increase the robustness and reduce the information redundancy among the calculated variables, we developed a 2-step variable selection procedure. Specifically, considering the separability of a single variable for the different forest management types and the cooperative effect of the variables with high separability values, the Fisher's discriminant ratio (FDR, [28]) and recursive feature elimination (RFE, [29]) methods were further applied for variable selection. Finally, we selected 20 of the 124 variables to train the random forest models.

Given that the variables related to growth characteristics were calculated using different algorithms for 2001 to 2003 and 2004 to 2020, we trained 2 random forest models for each continent to generate the annual forest management maps (Materials and Methods and Supplementary Text 3).

For period 1 (2004 to 2020), a set of global reference samples in 2015 was collected, including samples of NRF-NM (27,397), NRF-WM (60,871), $PF_{r>15}$ (7,360), $PF_{r\leq 15}$ (17,566), oil palm plantation (8,750), and agroforestry (24,334) provided by Lesiv et al. [11], and non-forest (3,417) provided by Liu et al. [30] (Table S19). Then, 80% of the labeled global reference samples and 20 selected variables for 2015 were used as training data for the random forest model to identify the forest management types from the time-series observations. Given that the sensor used to obtain the imagery has not changed and provided consistent data, the trained random forest model was applied to observations from other years to generate the annual forest management maps for 2004 to 2020.

For period 2 (2001 to 2003), we first determined the unchanged pixels combining the forest management maps for 2004 to 2020 and change detection results from continuous change detection and classification (CCDC, [31]) and structural change break point (SCBP) algorithms for 2001 to 2004. We then randomly selected 500 unchanged pixels for each forest management type on each continent and each nominal year for 2001 to 2003, which yielded a total of 63,000 unchanged pixels worldwide. Finally, we constructed a temporal random forest model for each continent that was re-trained using 80% of the selected unchanged pixels with 20 re-selected variables, to predict the changed pixels and construct the forest management maps for 2001 to 2003. Post-processing using a temporal filter and logical reasoning was further undertaken to increase the spatiotemporal consistency of the annual forest management maps (Supplementary Text 3 and Table S20).

Variable selection for the random forest model

Based on previous studies, we extracted 124 variables for classification of the forest management types. All variables were applied to a unified Eckert 4 equal area projection at a resolution of 250 m. We now use the variable extraction procedure for 2015 as an example (Table S20) to describe the extracted

variables in detail. Based on the similar composition of forest management types on a regional scale, we extracted geographic location factors as variables for the identification of different forest management types [32]. For the growth characteristics, we calculated the temporal changes, including intra-annual and seasonal variations of vegetation indices for the 5 years (2011 to 2015) preceding the nominal year (2015) to depict the differences between the forest management types. The distribution characteristics of the different forest management types result in the smoothness of the local images being different, which can be quantified by texture variables. In addition, human accessibility affects forest management activity, especially for planted forests, oil palm plantations, and agroforestry. Therefore, we extracted indicators of human activity from the global terrestrial Human Footprint dataset, as well as terrain-related indicators from GMTED2010, to provide auxiliary information on the classification of forest management types [32]. The variable extraction procedure for the other years during the period 2001 to 2020 was the same as for 2015. However, variables of growth characteristics for the nominal years of 2001 to 2003 were calculated using the 5-year MOD13Q1 imagery after the given nominal year.

Although the extracted variables depict the differences between the forest management types from a range of perspectives, there is some redundancy of information between these variables. If all the variables were input into the random forest model, then this would increase the uncertainty of the model and computational complexity. Therefore, we undertook a 2-step procedure to select the variables for the random forest model. We first calculated FDR for each variable to consider the separability of a single variable for the different forest management types [28]. We then applied the RFE algorithm [29] to assess the cooperative effect of the variables with high FDR values, to select the final variables for the forest management classification model. Detailed information regarding the selection of variables is presented in Supplementary Text 2.

Model training and validation

To ensure that the classification parameters were correctly tuned to the regional characteristics, and increase the sensitivity of the classification model to the training samples, we carried out a classification procedure for each continent. For each period, the random forest model was trained using 80% of the samples and the 20 variables selected for each continent. Specifically, for period 1 (2004 to 2020), a total of 149,695 global reference samples including samples of NRF-NM (27,397), NRF-WM (60,871), $PF_{r>15}$ (7,360), $PF_{r\leq 15}$ (17,566), oil palm plantation (8,750), and agroforestry (24,334) provided by Lesiv et al. [11], and non-forest (3,417) provided by Liu et al. [30] (Table S19) were applied to train the random forest model in each continent. For period 2 (2001 to 2003), a total of 63,000 samples derived from the initial annual forest management maps during 2004 to 2020 and change detection results during 2001 to 2003 were applied to train the random forest model in each continent. Given that the random forest model is largely insensitive to its hyper-parameters [33], this study referred to hyper-parameters applied in [34] and set the *Ntree* and *Mtry* values of the model for each continent to 100 and the default value (the square root of the total number of input features), respectively. To verify the robustness of the proposed mapping procedure, we carried out an accuracy assessment through an inter-comparison with available forest maps and validated

using 20% of the reference samples and samples compiled from previous studies. The accuracy was quantified with the confusion matrix, including the producer's accuracy, user's accuracy, overall accuracy (OA), and kappa coefficient. Detailed information about the validation of the annual forest management maps can be found in Supplementary Text 4.

Estimates of annual biomass carbon stocks

We estimated the biomass (above- and belowground) carbon stocks in different forest management types by co-locating the annual forest management maps and the annual corresponding biomass carbon density maps of Xu et al. [35]. The carbon density maps provided the annual global terrestrial live biomass carbon density from 2000 to 2019 at 10 km spatial resolution. The biomass carbon density maps were derived using a spatiotemporal random forest model combined with true measures of aboveground and belowground biomass and environmental factors extracted from multi-source data. The true measures of biomass were obtained by constructing allometric models between Lorey's height derived from spaceborne Geoscience Laser Altimeter System product aboard the Ice, Cloud, and land Elevation Satellite and biomass values derived from the global inventory of plot data. To estimate the annual biomass carbon stock of different forest management types, the biomass carbon density maps were firstly harmonized to a unified Eckert 4 equal area projection and resampled into a common spatial resolution of 250 m using the cubic convolution method. Then, the annual biomass carbon density maps were converted to the biomass carbon stock at the pixel scale by multiplying the area of a single pixel ($250 \text{ m} \times 250 \text{ m}$, $62,500 \text{ m}^2$). Finally, for each year, we summed the biomass carbon stock of each forest management type pixels to obtain the biomass carbon stocks in each forest management type, and the total biomass carbon stored in the forests was obtained by adding up the biomass carbon stored in different forest management types.

Results

Distribution of global forest management types

In general, the spatial distribution of different forest management types exhibits uneven patterns in the 6 continents (Africa, Asia, Europe, North America, Oceania, and South America) (Fig. 1A and Fig. S2). The spatial distribution of NRF is basically the same as that of forest, because NRF represents >80% of the global forest area. The NRF is mainly distributed in the tropical regions of South America, Central Africa, and Southeast Asia; the northern regions of Russia and Canada; and the Pacific and Atlantic coasts. In terms of the fine composition of NRF, NRF-NM is mainly distributed in tropical rainforest and high-latitude regions of the Northern Hemisphere, and NRF-WM is mainly patchily distributed around other forest management types globally, especially in the middle- and high-latitude regions of the Northern Hemisphere (Fig. 1A). The planted forest is mainly distributed in the middle- to high-latitude regions of the Northern Hemisphere and middle- to low-latitude regions of the Southern Hemisphere. $PF_{r>15}$ is mainly distributed in countries in southeastern North America, Europe, and Asia, and $PF_{r\leq 15}$ is mainly distributed in mid-latitude regions of the Southern Hemisphere, and in East and Equatorial Asia. Oil palm plantations are mainly distributed in Southeast Asia, especially Indonesia, Malaysia, Philippines, and Thailand. Agroforestry is mainly distributed in middle- and low-latitude regions (Fig. 1A).

To verify the performance of the generated annual maps, we further validated our maps at point and spatial scale using dataset described earlier. Specifically, we first evaluated the performance of the random forest model and the accuracy of the annual forest management maps using 20% of the global reference samples and samples collected in previous studies, respectively. The estimated OA was 82.25% for the model constructed for 2001 to 2003 (Table S1) and 74.45% for the model constructed for 2004 to 2020 (Table S2). For the annual forest management maps, we verified the forest identification, particularly the distinction between tree plantations and natural forests, because the samples collected provide information about natural forests and tree plantations, but lack information regarding the fine composition of forest management types (Supplementary Text 4). Here, the tree plantation includes $PF_{r>15}$ and $PF_{r\leq 15}$, oil palm and agroforestry, and the natural forest includes NRF-NM and NRF-WM, and forest denotes all types of forest management. To evaluate the accuracy of forest identification, our forest maps were validated using samples presented in previous studies [36–39]. The estimated OA values are >93.28% (Table S3). For the tree plantation–natural forest maps, the estimated OA values are >75.55% at the global and regional scales (Tables S4 to S9). In addition, our forest management map in 2015 exhibited a more robust performance than FML_v3 when validated using samples in 2015 interpreted using high spatial resolution (<1 m) Google Earth satellite images, around the global scale and in China [40] and Tanzania [41] (Tables S4, S5, and S8–S10).

Second, we compared our forest management maps with official statistical data of the UN Food and Agriculture Organization (FAO) and other available data products. For different spatial land cover maps, we determine the area belonging to forest categories. The specific second-level classes belonging to forests in different land cover products are shown in Table S11. As shown in Figs. S3 to S5, our maps exhibit similar spatial patterns of forest, NRF, and planted forest as other data products [11,13,21,34,42,43]. In addition, the estimated annual NRF and planted forest areas in this study are consistent with those reported by the FAO (Fig. S6). However, the annual forest areas obtained from the different data products are inconsistent, which may be due to the source data and methodologies used to identify the forest [34]. The estimated annual forest areas in this study are broadly consistent with GLC_FCS30 from Zhang et al. [34], which has a more accurate representation of the spatial distribution of forests globally than other forest maps [34]. Furthermore, the annual and expanded area of planted forest from 2001 to 2020 is comparable with those reported by FAO [23]. Detailed information about the validation results on a point scale can be found in Supplementary Text 4 (Figs. S3 to S10 and Tables S1 to S10).

The validation results on a point-scale and inter-comparison with other data products show that the forest management maps generated in this study accurately represented the global spatiotemporal variations of forest management types. Therefore, the spatiotemporal analysis of the fine composition of forest and biomass carbon estimation based on the generated annual forest management maps is reasonable.

Spatiotemporal changes in global forest management types from 2001 to 2020

The global forest area has decreased by $212.73 \times 10^4 \text{ km}^2$ since 2001, which is equivalent to 4.59% of the global forest area in 2001 (Fig. S11). This decrease was entirely due to NRF (NRF-NM and NRF-WM), especially in Asia (44%) and North

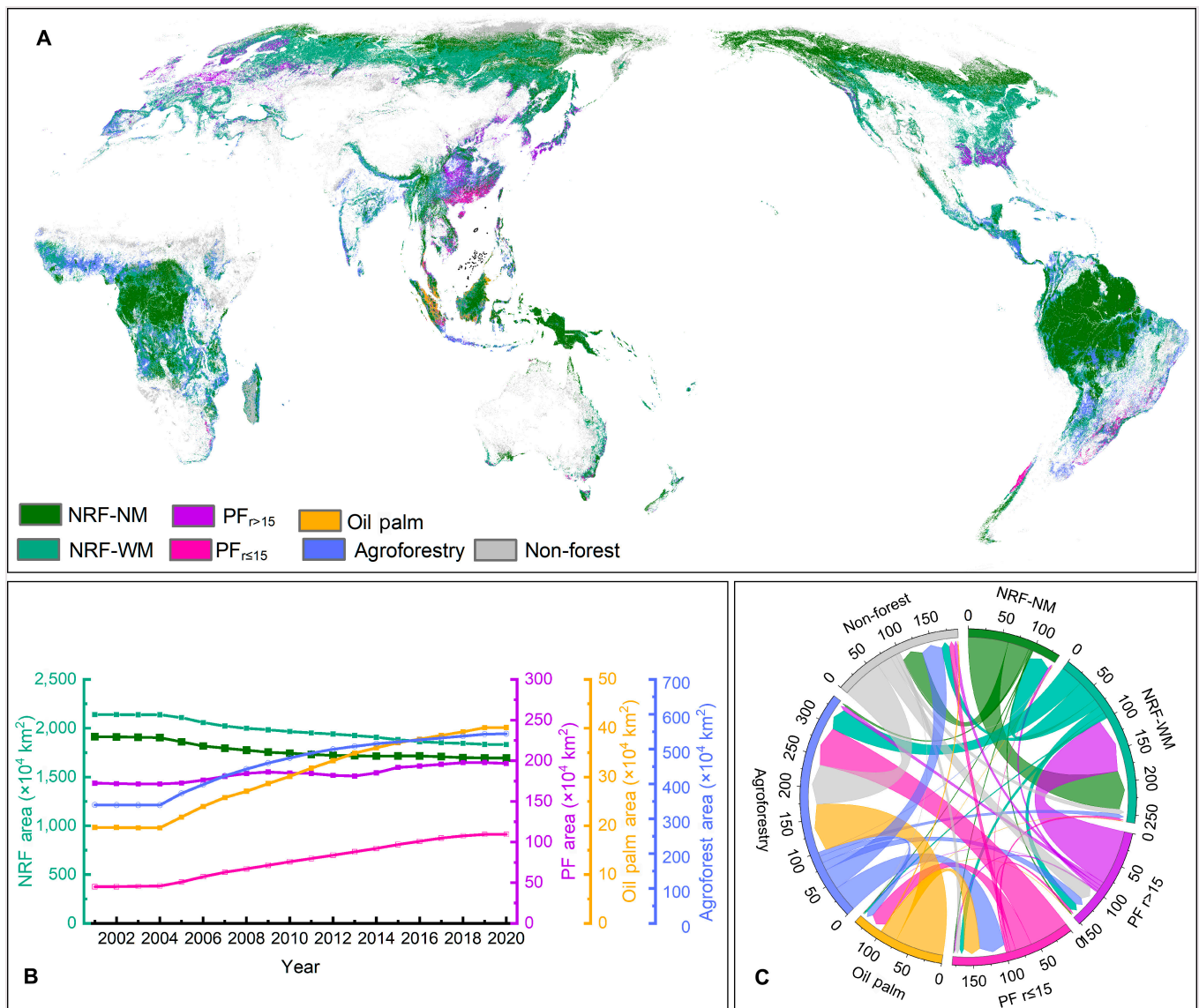


Fig. 1. Spatial distribution, variations, and transitions of different forest management types from 2001 to 2020. (A) Spatial distribution of different forest management types in 2015. (B) Annual areas of forest management types from 2001 to 2020. (C) Transitions in forest management types from 2001 to 2020. For a better display, the values in the chord diagram in (C) were normalized as the area proportion contributed by other forest management types in the increased area of a certain type of forest management. Detailed area values are listed in Table S12. Taking the increase of NRF-NM as an example, the values were calculated as the area proportion of NRF-WM, $PF_{r>15}$, $PF_{r\leq 15}$, oil palm plantations, and agroforestry converted to NRF-NM to that of the total increasing in NRF-WM, respectively.

America (29%) (Fig. S11). Furthermore, NRF was the main component of forests, except in Europe, where the forests consist mainly of NRF-WM and $PF_{r\leq 15}$ (Fig. S12). The proportion of NRF in forests decreased on each continent (Fig. S12A to F).

In terms of the fine composition of the forest, the global NRF decreased by $526.08 \times 10^4 \text{ km}^2$, totally contributed by NRF-WM (58.32%) and NRF-NM (41.68%). The decrease in NRF-NM occurred mainly in Asia (55.62%) and North America (28.42%), whereas that of NRF-WM occurred mainly in South America (41.23%), Africa (24.04%), and Asia (17.55%). Moreover, the interconversions between naturally regenerated forests that are unmanaged and managed accounted for 48.95% and 40.70% of each other's area losses, respectively. In addition, about 32.37% and 12.17% of the decrease in NRF-NM and NRF-WM was due to conversion to non-forest, respectively (Fig. 2A and B). On a country scale, the decrease in NRF-NM was greatest

in Russia, followed by Canada and the United States, while Brazil underwent the largest decrease in NRF-WM (Fig. 3 and Fig. S13A and B).

Substantial expansion occurred in PF ($PF_{r>15}$ and $PF_{r\leq 15}$; an increase of $88.74 \times 10^4 \text{ km}^2$), oil palm plantations ($20.50 \times 10^4 \text{ km}^2$), and agroforestry ($204.13 \times 10^4 \text{ km}^2$), which offset 59.56% of the forest loss caused by the decrease in NRF. During 2001 to 2020, the global area of $PF_{r\leq 15}$ increased by a factor of 2.4 (Fig. 1B), and the expanded area has contributed 72.65% of the global PF expansion, which occurred mainly in Asia (61.19%) and South America (30.22%) (Fig. S12). This expansion occurred mainly in Brazil, Chile, China, Indonesia, Vietnam, Thailand, and Australia (Fig. S14A). These 7 countries together contributed >74% of the corresponding annual global $PF_{r\leq 15}$ areas and >86% of the corresponding expanded $PF_{r\leq 15}$ areas (Fig. 3). In contrast, the global expansion of $PF_{r>15}$ occurred mainly in Europe (76.45%), while

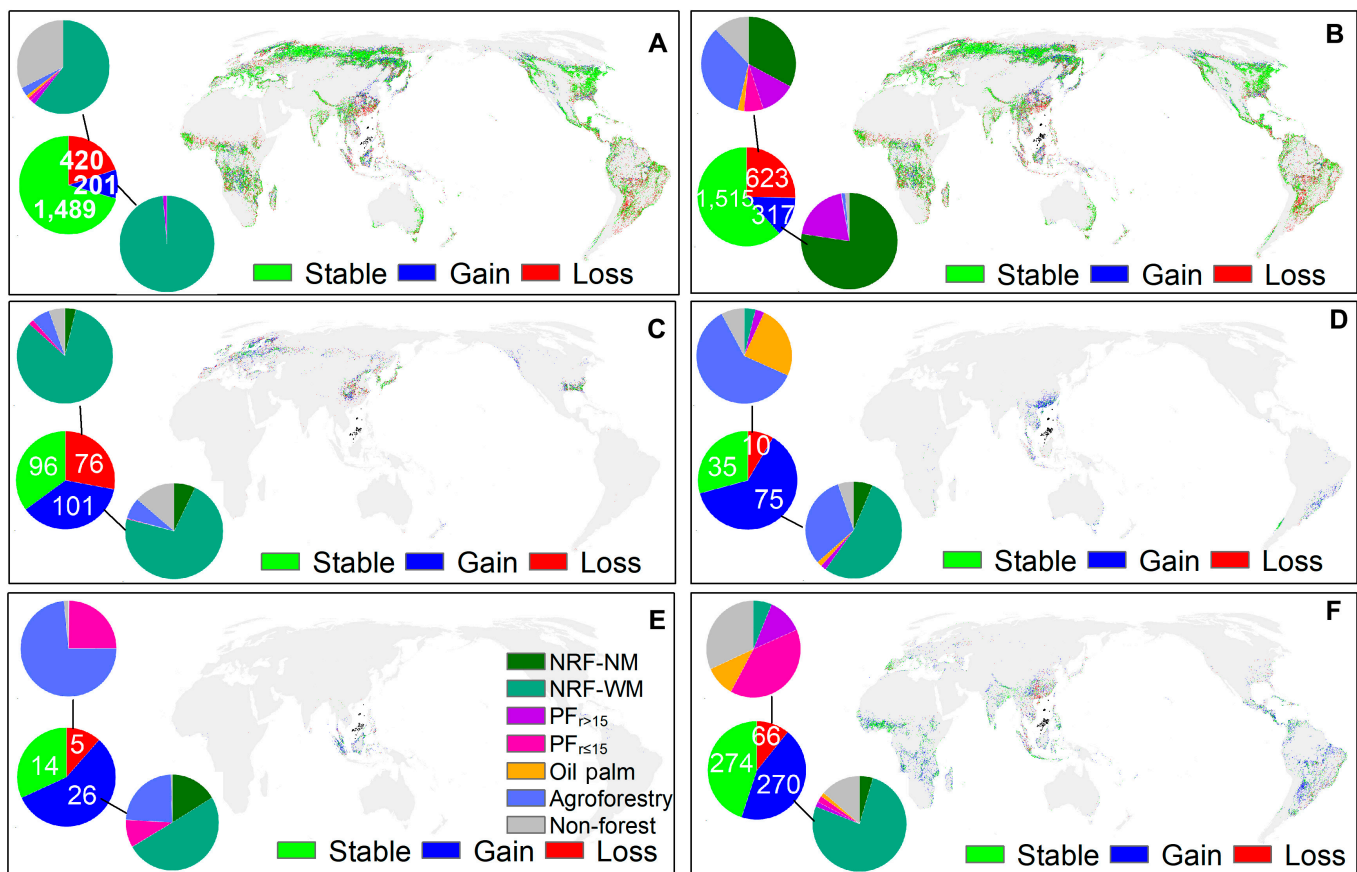


Fig. 2. Changes in the spatial pattern of forest management types from 2001 to 2020. (A) NRF-NM; (B) NRF-WM; (C) $PF_{r>15}$; (D) $PF_{r\leq 15}$; (E) oil palm plantations; (F) agroforestry. The gains and losses denote conversions between the forest management types. Taking NRF-NM as an example, a loss represents a conversion from NRF-NM to non-NRF-NM, while a gain denotes a conversion from non-NRF-NM to NRF-NM

the largest expansion occurred in the United States ($5.42 \times 10^4 \text{ km}^2$; 22.30%) (Fig. S11 and Fig. 3).

The global increase in the area of oil palm plantations is equivalent to the global oil palm plantations area in 2001, due to an increase in Asia (91.52%) (Figs. 1B and 2). This expansion occurred mainly in countries in Equatorial Asia, such as Indonesia (62.93%), Malaysia (20.0%), Philippines (6.34%), and Thailand (1.95%) (Fig. S14B). These 4 countries contributed >90% of the annual global oil palm plantation area (Fig. 3). The expanded area of agroforestry was equivalent to 60.07% of the agroforestry area in 2001 ($339.82 \times 10^4 \text{ km}^2$), and was mainly in South America (42.43%) and Africa (34.66%). In particular, Brazil had the most substantial agroforestry expansion of $30.81 \times 10^4 \text{ km}^2$, accounting for 15.09% of the annual global agroforestry area (Fig. S14C).

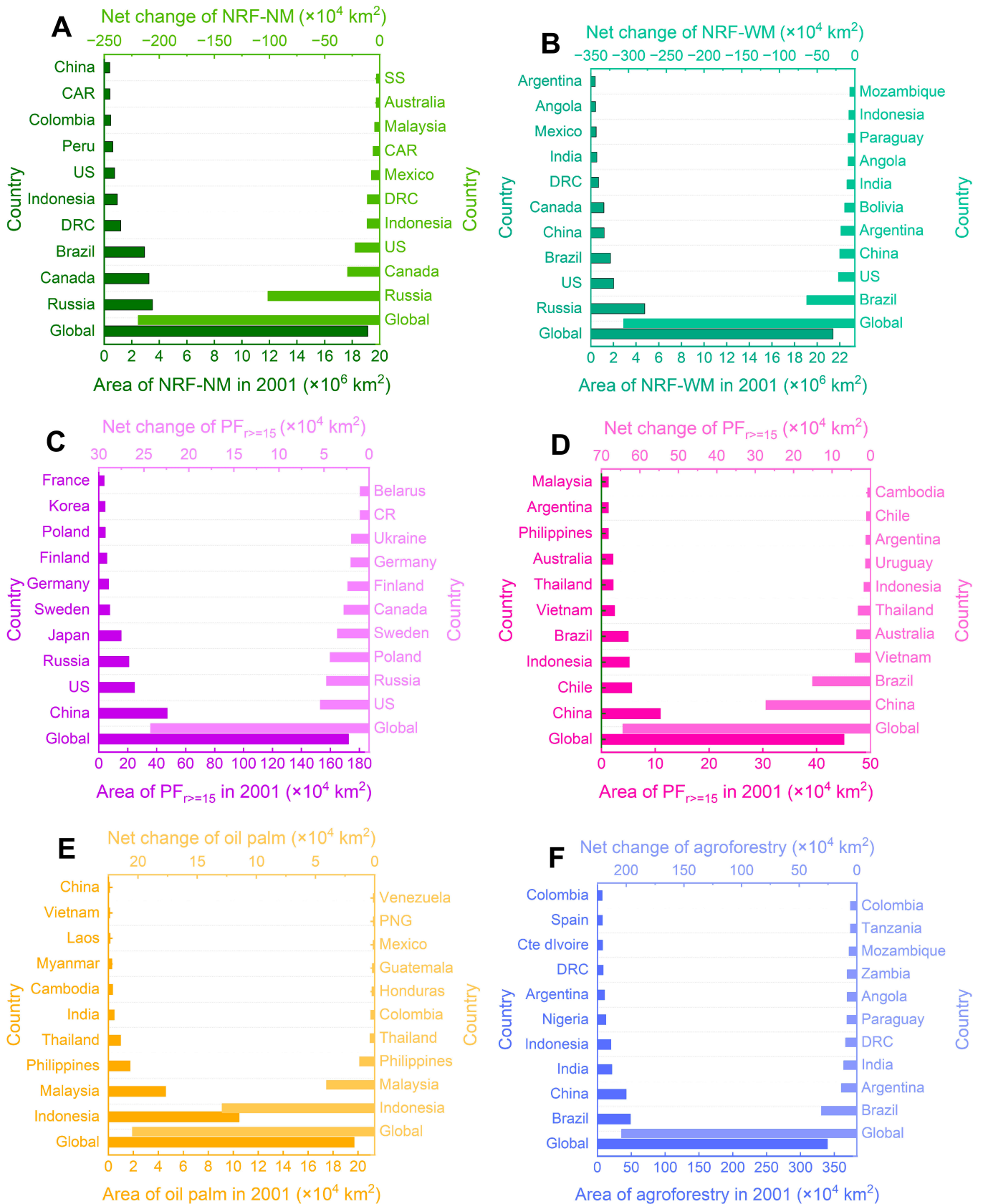
The expansion of different forest management types was uneven in nature. In detail, the increase in $PF_{r>15}$ and agroforestry was mainly in the regions where NRF-WM and non-forest were replaced, while the increase in $PF_{r\leq 15}$ and oil palm plantations was mainly in regions where NRF-WM and agroforestry were replaced (Table S12).

Changes in biomass carbon due to changes in forest management types

We estimated the biomass (above- and belowground) carbon stock in different forest management types by co-locating the annual maps and the corresponding biomass carbon density

maps of Xu et al. [35]. In general, the biomass carbon stocks in forest decreased from 282.78 Pg C in 2001 to 279.02 Pg C in 2020 (Fig. 4A). The biomass carbon stock in NRF decreased by 16.44 Pg C, with the loss in NRF-WM dominating this decrease (65.68%; 10.80 Pg C), followed by NRF-NM (34.32%; 5.64 Pg C) (Fig. 4B). The loss of biomass carbon stock in NRF-NM was dominated by Asia (87.59%), while that of NRF-WM was mainly due to South America (51.94%) and Africa (19.54%). In contrast, the biomass carbon stocks in PF ($PF_{r>15}$ and $PF_{r\leq 15}$; 4.52 Pg C), oil palm plantations (0.89 Pg C), and agroforestry (7.28 Pg C) increased by 12.68 Pg C, which offset 77.13% of the biomass carbon loss in NRF (Fig. 4B). The increase in biomass carbon stock of $PF_{r\leq 15}$ contributed 66.26% of the corresponding increase in PF (Fig. 4B). The increase of biomass carbon stock in $PF_{r>15}$ was mostly and equally contributed by Europe and North America, while that of $PF_{r\leq 15}$ was mainly contributed by Asia (64.21%), South America (20.07%), and Oceania (13.04%). Like the oil palm plantation expansion, the gain of this biomass carbon stock was almost solely in Asia. The gain of biomass carbon stock in agroforestry was mainly in Africa and South America, which had similar percentage increases.

We investigated the temporal variations of biomass carbon stock in planted forest and its contribution to the overall forest. In general, the uneven pattern of average biomass carbon stock in planted forests globally resembles that of its contribution to forest biomass carbon stock, and exhibits an opposite trend to



Downloaded from https://spj.science.org on March 15, 2024

Fig. 3. Ranking of the top 10 countries with the largest forest area in 2001 and the top 10 countries with substantial area changes in each forest management type. (A) NRF-NM; (B) NRF-WM; (C) $PF_{r>=15}$; (D) $PF_{r<=15}$; (E) oil palm plantations; (F) agroforestry. For each plot, the bottom-x and left axis denote the area in 2001 for each forest management type, while the top-x and right axis denote the net change area from 2001 to 2020 for each forest management type. Notes: DRC = Democratic Republic of the Congo; CAR = Central Africa Republic; CR = Czech Republic; US = the United States; PNG = Papua New Guinea; SS = South Sudan.

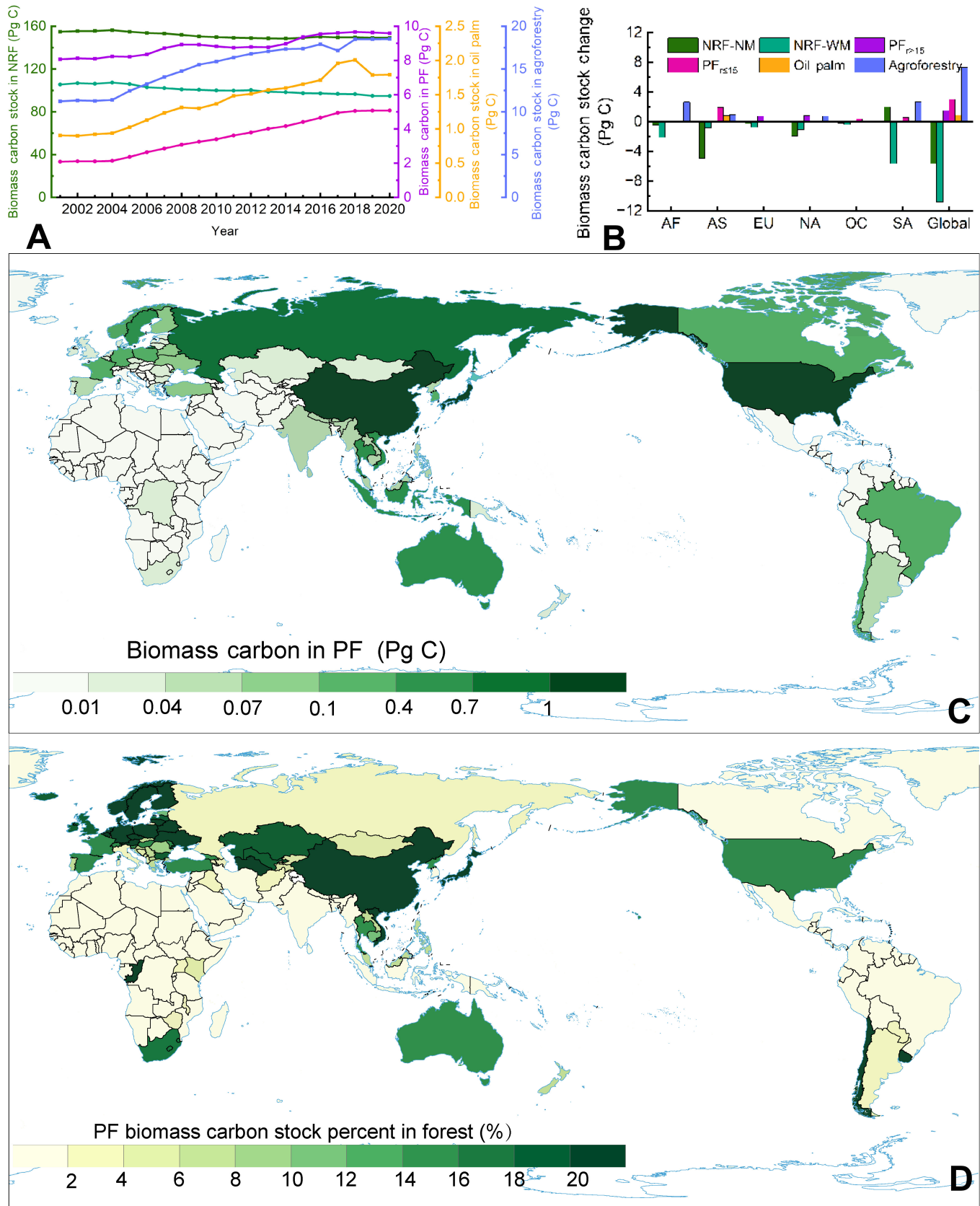


Fig. 4. Biomass carbon stock changes from 2001 to 2020. (A) Global biomass carbon stock change for each forest management type during 2001 to 2020. (B) Biomass carbon stock change for each forest management type from 2001 to 2020 on a continent scale. (C) Average biomass carbon stock in PF from 2001 to 2020. (D) The average proportion of biomass carbon stock in PF relative to forest. For the x-axis in (B), AF, AS, EU, NA, OC, and SA denote Africa, Asia, Europe, North America, Oceania, and South America, respectively.

the temporal variations (Fig. 4C and D and Fig. S16). Strong temporal variations ($cv > 1$) were most pronounced in countries in northern Africa (Fig. S16A), which have a low biomass carbon stock in planted forests (Fig. 4C) and small contributions to forest biomass carbon stock (Fig. 4E). Weak temporal variations ($cv < 0.1$) mainly characterize in Asian countries, particularly in China, Russia, and Japan, and North American countries such as the United States (Fig. S16). These countries have a high average biomass carbon stock (>0.7 Pg C) and moderate (2%–20%) or high ($>20\%$) contributions to the forest biomass carbon stock. Moderate temporal variations ($cv = 0.1$ to 1) were common in most countries, and these countries have low to moderate biomass carbon stocks in PF and contributions to the forest biomass carbon stock (Fig. 4C and D and Fig. S16).

Changes in the area and corresponding biomass carbon stocks of different forest management types in specific countries

To better understand the regional changes in the forest management area and the corresponding biomass carbon stock from 2001 to 2020, we selected 4 countries with larger area variations (China, Russia, the United States, and Brazil) to further explore the spatiotemporal variations in the different forest management types, and transitions between these types.

Since 2001, a substantial decrease in NRF has occurred in Russia and Brazil, mainly from NRF-NM and NRF-WM, respectively. The decrease in NRF-NM in Russia is estimated to be the largest ($101.56 \times 10^4 \text{ km}^2$), and accounts for 46.31% of the global loss of NRF-NM (Fig. 3). This loss resulted in a decrease of corresponding biomass carbon stock that accounts for 60.29% of the global decrease (Table S13). The interconversions between

NRF-WM and NRF-NM reduced the decrease in NRF-NM by about $20 \times 10^4 \text{ km}^2$, and the conversion of NRF-NM into non-forest accounted for most of the decrease in NRF-NM (Fig. 5, Table S14). In addition, the area changes resemble those reported by the FAO (Fig. S14b). The forest area of the Brazilian Amazon, as estimated in the present study, varied from 369.38 to $368.98 \times 10^4 \text{ km}^2$ during 2007 to 2010, which is similar to the range of 377 to $375 \times 10^4 \text{ km}^2$ reported by Qin et al. [44].

Brazil contributed the largest decrease to NRF-WM and accounted for 20.87% of the global loss in NRF-WM, leading to a decrease of biomass carbon stock (3.31 Pg C), which is 33.69% of the global total (Fig. 3 and Table S13). The area loss of NRF-WM in Brazil, China, and the United States was broadly similar (Tables S15 to S17). However, the fate of the lost NRF-WM areas was different in these 3 countries. The lost NRF-WM was mainly converted to oil palm plantations ($34.05 \times 10^4 \text{ km}^2$), NRF-NM ($18.74 \times 10^4 \text{ km}^2$), non-forest ($12.20 \times 10^4 \text{ km}^2$), and $PF_{r \leq 15}$ ($9.27 \times 10^4 \text{ km}^2$) in Brazil; $PF_{r > 15}$ and $PF_{r \leq 15}$; $23.64 \times 10^4 \text{ km}^2$, NRF-NM ($19.30 \times 10^4 \text{ km}^2$), and oil palm plantations ($11.75 \times 10^4 \text{ km}^2$) in China; and non-forest and $PF_{r > 15}$ in the United States (Tables S15 to S17).

In the past 2 decades, China and Brazil have experienced the most substantial increase in planted forest, reaching 22.80×10^4 and $14.96 \times 10^4 \text{ km}^2$, accounting for 25.69% and 16.86% of the increase in global planted forest, respectively. These increases have led to a 1.22 and 0.45 Pg C increase in biomass carbon stock in China and Brazil, respectively. The expanded $PF_{r \leq 15}$ contributed most to the increase in planted forest, with that in China and Brazil accounting for 42.20% and 23.43% of the increase in global $PF_{r \leq 15}$, respectively (Fig. 3). The expansion of $PF_{r \leq 15}$ led to an increase in biomass carbon stocks in China and Brazil that account for 46.62% and 15.12% of the global

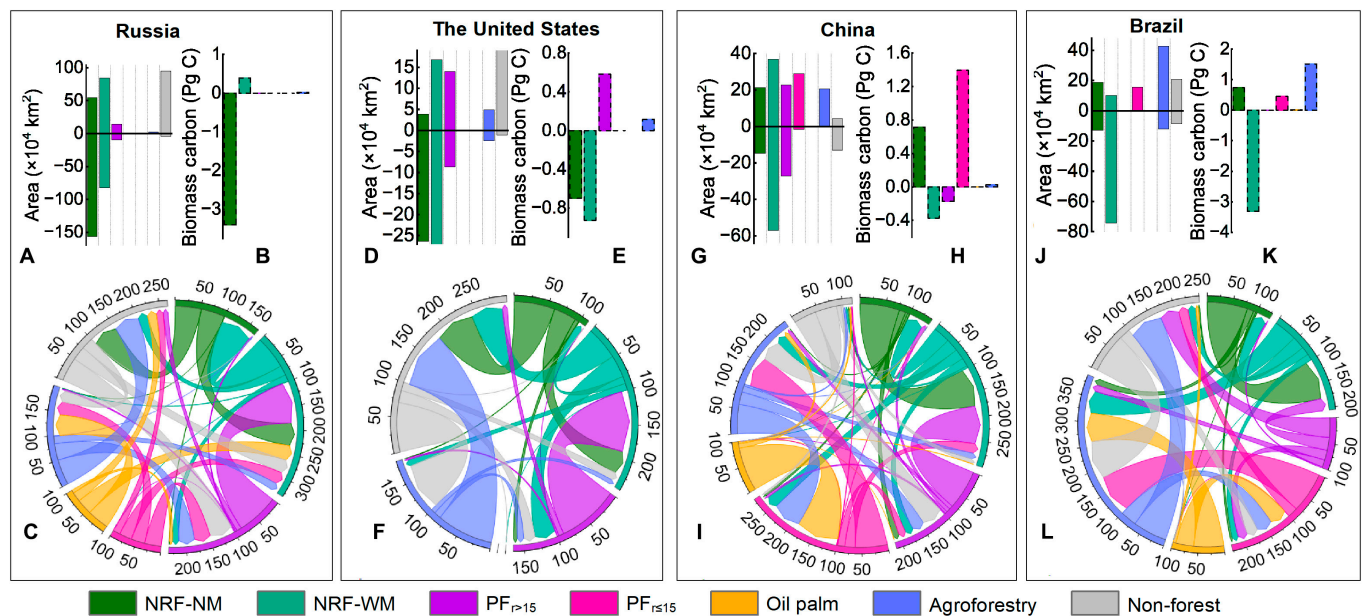


Fig. 5. Changes in area and corresponding biomass carbon stock, and the transitions between forest management types in specific countries from 2001 to 2020. (A, D, G, J): Area changes of different forest management types in Russia, the United States, China, and Brazil, respectively. (B, E, H, K): Biomass carbon stock changes of different forest management types in Russia, the United States, China, and Brazil, respectively. (C, F, I, L): Interconversion among different forest management types in Russia, the United States, China, and Brazil, respectively. For a better display, the values in the chord diagram in (C), (F), (I), and (L) were normalized as the area proportion contributed by other forest management types in the increased area of a certain type of forest management. Detailed area values are listed in Tables S14, S16, S17, and S15. Taking the increase of NRF-NM as an example, the values were calculated as the area proportion of NRF-WM, $PF_{r > 15}$, $PF_{r \leq 15}$, oil palm plantations, and agroforestry converted to NRF-NM to that of the total increasing in NRF-WM, respectively.

increase of biomass carbon stock in $PF_{r \leq 15}$, respectively (Table S13). In addition, the expansion of $PF_{r \leq 15}$ in both China and Brazil was mainly due to the decrease of NRF-WM and agroforestry (Tables S15 and S7). In China, the expanded area of planted forest during 2001 to 2020 was 18.62% lower than that reported by FAO [23]. In addition, the expanded area and biomass carbon stock increase during 2001 to 2013 was 7.45% and 32.21% higher than that reported by Zhang et al. [45] during 1999 to 2013 using forest inventory data, respectively. In Brazil, the expansion of planted forests is slightly greater than that reported by FAO ($7.20 \times 10^4 \text{ km}^2$) (Fig. S17C). This discrepancy is due to different source data and methodologies.

A total of 5.42×10^4 and $4.72 \times 10^4 \text{ km}^2$ of planted forest expansion occurred in the United States and Russia, respectively, which is comparable to that reported by the FAO (Fig. S17). In addition, the planted forest expansion led to a 0.58 and 0.17 Pg C increase in biomass carbon stock in the United States and Russia, respectively. An increase in $PF_{r > 15}$ was almost solely responsible for the planted forest expansion in both the United States and Russia, which replaced NRF-WM (Table S14 and S16).

Discussion

Advance in the methodology

This study presents several advances in global forest mapping. We finely classified the forest toward a management way using random forest and change detection algorithms.

First, variable extraction and selection. To depict the differences among forest management types, we constructed a series of variables including variables of growth characteristics, local textural information, and human influences based on multi-source dataset. For the variables related to growth characteristics in particular, we calculated the slope of the vegetation indices versus the image acquisition date. Generally speaking, different forest management types have different growth characteristics. For example, planted forests oriented by timber production grow fast and get matured in a short period, while natural regeneration forests require a longer time to mature. Also, planted forests are distributed over large areas and with single tree species, leading to uniform and low-contrast visual patterns due to the unified height and density of tree crown cover, and thereby the texture differences with natural regeneration forests. In addition, other variables also depict the differences in forest management types. To filter the variables favoring forest management type classification, the FDR and RFE algorithms were applied for variable selection. The FDR estimates the separability of an independent variable with respect to the classification target by considering the relationship between intra- and inter-class variances, while the RFE algorithm searches for an optimal subset of variables. The combination of the 2 algorithms can effectively reduce the information redundancy and filter the variable that is conducive to distinguishing forest management type.

Second, we applied random forest and change detection algorithms to generate the annual fine composition of forests toward a management perspective. The random forest is highly effective in handling high-dimensional data and preventing overfitting by introducing randomness in sampling and variable selection, and has been widely applied in forests [30], agriculture [29], etc. The non-linear response of vegetation growth to environmental variables is precisely where random forests excel. In addition, change detection algorithms are also widely applied in detecting

disturbances such as deforestation, and reforestation practices. However, change detection results have marked spatial variations based on different change detection algorithms [46]. In this study, we combined the results of 2 change detection algorithms (CCDC and SCBP) to increase the robustness of change detection results. Combining random forest and change detection algorithms, the generated annual maps accurately represented the global spatio-temporal variations of forest management types.

Potential implications of the forest management maps

The net effect of different forest management types on restoring ecosystem services and addressing climate change has been difficult to assess in the absence of global maps of the fine composition of forests. The spatiotemporal patterns of forest management types obtained in this study enable us to evaluate the influence of different forest management types on ecosystem services, and the effectiveness of tree plantation-centered practices in mitigating climate change. Specifically, the annual forest management maps can be further applied to the following research aspects:

First, forest management. On a global scale, state-of-the-art products include FROM-GLC maps [47], GlobeLand30 maps [48], and GLC_FCS maps [34], none of which distinguished the fine composition of forests from a forest management perspective. The annual forest management maps obtained in the present study supplement the current land cover and use products. In addition, although the expansion of tree plantations (planted forests, oil palms, and agroforestry) offsets a large amount of the decrease in natural regeneration forests, this expansion has resulted in deforestation [49]. Previous studies have shown that mega-fires have been associated with the expansion of tree plantations [50,51]. Therefore, improvements in forest management practices, such as enhancing the protection of natural forests and tree plantations, as well as preventing potential risks associated with forest degradation and afforestation, are required.

Second, driven data for land surface process modeling. Forest management type altered the tree species and forest composition, which, in turn, affected the surface fluxes, such as latent heat flux, soil heat flux, net radiation flux, etc. However, the influences of the fine composition of forest on physical, biochemical, and ecological processes were insufficiently considered in land surface process models, especially the surface flux simulations. This insufficient consideration was mainly aroused from the limited spatially explicit information about forest management type. In this study, we generated long-term patterns of forest management types during 2001 to 2020 and provided detailed driven data for the surface process models to simulate or re-evaluate the carbon, water, and energy cycles, and further explore the biophysics and climate effects caused by forest composition variations.

Third, sustainable development goals. Forest is a vital component of ecosystems worldwide, and accounts for ~30% of the terrestrial land area. To mitigate climate change, reforestation and afforestation practices have been developed. However, the effectiveness of planted forests in climate change mitigation is poorly understood due to the lack of available forest management maps and biomass carbon datasets. The estimated increase in biomass carbon stock in tree plantations (planted forest, oil palm, and agroforestry) obtained in this study indicates that planted forests can contribute to climate change mitigation. This provides the impetus that could lead to the implementation of ambitious policy proposals related to tree plantations, such as the Bonn

Challenge, the Trillion Tree Initiative, and the United Nations Decade of Ecosystem Restoration [52]. The maps also provide supplementary information to support decision-making related to sustainable development and climate change mitigation.

Limitations and further improvements

This study documented the spatiotemporal pattern of the fine composition of global forests from the perspective of forest management, and quantified the annual biomass carbon stock in each forest management type. In general, the area of naturally regenerating forests is decreasing, whereas the area of planted forests, oil palm plantations, and agroforestry is increasing. This expansion has mostly offset the decreasing biomass carbon stock caused by the decrease in naturally regenerating forests.

However, there are limitations to our approach that require further research. First, we generated the annual forest management maps for 2001 to 2020 at a spatial resolution of 250 m. Fine-scale products should be further developed using imagery such as the Landsat archive to distinguish the forest management types more accurately. In addition, although the biomass carbon stock maps used in this study provide the annual spatial distribution of living vegetation, their coarse spatial resolution may introduce uncertainties to the estimates of biomass carbon stocks. However, this is the only product currently available that provides a long-term time series of biomass carbon densities. Future research should focus on forest management types and biomass carbon stocks on a finer spatial scale.

Conclusion

This study generated the annual global fine composition of forests from a forest management perspective during 2001 to 2020 based on random forest and change detection algorithms. Furthermore, we estimated the biomass carbon stocks in the different forest management types and investigated their temporal changes. The main conclusions were as follows: (a) Combining substantial validation results at the point and spatial scales indicated that the resultant annual maps accurately represented the global spatiotemporal variations of different forest management types. (b) The expansion of planted forests, oil palm plantations, and agroforestry offset over half of the loss of forest area and biomass carbon stock due to the degradation of naturally regenerated forests. (c) The expansion of planted forests with rotation ≤ 15 years contributed 72.73% of that of global planted forests, and China alone dominated this expansion. (d) Except for managed natural regeneration forests, reforestation also explained the extensive expansion of planted forests with rotation >15 years and agroforestry, while agroforestry shrinkage contributed to abundant expansion of planted forests with rotation ≤ 15 years and oil palm. Results from this study are beneficial for re-evaluating the influences of forest degradation, afforestation, and reforestation practices for climate change mitigation.

Acknowledgments

Funding: This research was supported by the BNU-FGS Global Environmental Change Program (grant 2023-GC-ZYTS-01), the High-Resolution Earth Observation Major Special Aerial Observation System (grant 30-H30C01-9004-19/21), and the State Key Laboratory of Earth Surface Processes and Resource Ecology (grant 2023-KF-02).

Author contributions: B.H. and L.G. designed the research; H.X. performed the analysis and wrote the draft. All authors contributed to the interpretation of the results and the writing of the paper.

Competing interests: The authors declare that they have no competing interests.

Data Availability

The annual maps of forest management types generated in this study can be freely downloaded from <https://zenodo.org/records/10478678> or <https://data.tpd.ac.cn/zh-hans/data/7f349001-ef38-43ee-9f8f-4722d986a1c1>. The source data used for generating the FP maps in this study included the imagery of NDVI and EVI during 2013 to 2017, backscatter coefficients observations of ALOS PALSAR in 2015, and Global Multi-resolution Terrain Elevation Data 2010 (GMTED2010); the forest map provided by Shimada et al. [43], the global land cover MCD12Q1, and the forest gain map provided by Hansen et al. [53] on the Google Earth Engine are available at <https://earthengine.google.com/>. The SDPT VERSION 1.0 provided by Harris et al. [22] is available at <https://data.globalforestwatch.org/datasets/224e00192f6d408fa5147bbfc13b62dd>. The Intact Forest Landscapes (IFL) dataset provided by Potapov et al. [12] is available at <https://intactforests.org/data.ifl.html>. For the spatial maps, the FP map provided by Schulze et al. [13] is available at <https://www.environmentalgeography.nl/site/data-models/data/forest-classes-and-uses/>. The reference samples provided by Fagan et al. [15] are available at <https://data.globalforestwatch.org/content/pantropical-tree-plantation-expansion-2000-2012/about>. The GLC_FCS data are available at <https://doi.org/10.5281/zenodo.3986872>. The CCI land cover maps are available at <http://maps.elie.ucl.ac.be/CCI/viewer/download.php>. The global forest management map in 2015 provided by Lesiv et al. [11] is available at <https://zenodo.org/record/4541513#.ZD99FHZByUk>. For the reference samples, the global land cover validation dataset for 2010 [36] is available at <http://data.ess.tsinghua.edu.cn/>. The global land cover validation dataset for 2015 provided by Liu et al. [30] is available at <https://doi.org/10.5281/zenodo.3551995>. The land cover validation dataset of Central Asia provided by Hu et al. [38] is available at https://drive.google.com/drive/folders/1SLr_L-G72t6CWHHKnHgAt-F5G1Gn9t_am. The reference samples in China provided by Wu et al. [40] are available at <https://www.scidb.cn/en/detail?dataSetId=a857a0fb2a144168ab755fd3889f51e6>. The global land cover reference samples provided by Fritz et al. [39] are available at <https://doi.pangaea.de/10.1594/PANGAEA.869680>. The reference samples in Chile provided by Adison et al. [54] are available at http://www.lepfor.ufro.cl/?page_id=530. The 4 validation samples dataset in Tanzania were provided by Koskinen et al. [41], and the reference point dataset is available at <https://doi.pangaea.de/10.1594/PANGAEA.894887>, the training dataset is available at <https://doi.pangaea.de/10.1594/PANGAEA.894889>, the validation dataset is available at <https://doi.pangaea.de/10.1594/PANGAEA.894890>, and the validation dataset field dataset is available at <https://doi.pangaea.de/10.1594/PANGAEA.894891>. The biomass carbon density maps provided by Xu et al. [35] are available at <https://doi.org/10.5281/zenodo.4161694>.

Supplementary Materials

Supplementary data associated with this article can be found in Supplementary Materials. Supplementary Text 1 to 4

Figs. S1 to S18
 Tables S1 to S21
 References [55–59]

References

- Harris NL, Gibbs DA, Baccini A, Birdsey RA, Farina M, Fatoyinbo L, Hansen MC, Herold M, Houghton R, Potapov PV, et al. Global maps of twenty-first century forest carbon fluxes. *Nat Clim Chang*. 2021;11(3):234–240.
- Lu N, Tian H, Fu B, Yu H, Piao S, Chen S, Li Y, Li X. Biophysical and economic constraints on China's natural climate solutions. *Nat Clim Change*. 2022;12:847–853.
- Griscom BW, Adams J, Ellis PW, Houghton RA, Lomax G, Miteva DA, Schlesinger WH, Shoch D, Siikamäki JV, Smith P, et al. Natural climate solutions. *Proc Natl Acad Sci U S A*. 2017;114(44):11645–11650.
- Drever CR, Cook-Patton SC, Akhter F, Badiou PH, Chmura GL, Davidson SJ, Desjardins RL, Dyk A, Fargione JE, Fellows M, et al. Natural climate solutions for Canada. *Sci Adv*. 2021;7(23):eabd6034.
- Fargione JE, Bassett S, Boucher T, Bridgman SD, Conant RT, Cook-Patton SC, Ellis PW, Falcucci A, Fourqurean JW, Gopalakrishna T, et al. Natural climate solutions for the United States. *Sci Adv*. 2018;4(11):eaat1869.
- Barr CM, Sayer JA. The political economy of reforestation and forest restoration in Asia–Pacific: Critical issues for REDD+. *Biol Conserv*. 2012;154:9–19.
- Jonah B, Kalifi FG, Jens E, Max W, Austin KG, Fred S, Svetlana T, Potapov PV, Belinda M, Hansen MC, et al. Reductions in emissions from deforestation from Indonesia's moratorium on new oil palm, timber, and logging concessions. *Proc Natl Acad Sci U S A*. 2015;112(5):1328.
- Kezia G, Ingo S, Fran?ois B, Tesfaye W. Forest management type influences diversity and community composition of soil fungi across temperate Forest ecosystems. *Front Microbiol*. 2015;6:1300.
- Lewis SL, Wheeler CE, Mitchard ETA, Koch A. Restoring natural forests is the best way to remove atmospheric carbon. *Nature*. 2019;568(7750):25–28.
- Yu Z, Liu S, Wang J, Wei X, Schuler J, Sun P, Harper R, Zegre N. Natural forests exhibit higher carbon sequestration and lower water consumption than planted forests in China. *Glob Chang Biol*. 2019;25(1):68–77.
- Lesiv M, Schepaschenko D, Buchhorn M, See L, Düräue M, Georgieva I, Jung M, Hofhansl F, Schulze K. Global forest management data for 2015 at a 100m resolution. *Sci Data*. 2022;9:199.
- Potapov P, Hansen MC, Laestadius L, Turubanova S, Yaroshenko A, Thies C, Smith W, Zhuravleva I, Komarova A, Minnemeyer S, et al. The last frontiers of wilderness: Tracking loss of intact forest landscapes from 2000 to 2013. *Sci Adv*. 2017;3(1):e1600821.
- Schulze K, Malek Ž, Verburg PH. Towards better mapping of forest management patterns: A global allocation approach. *For Ecol Manag*. 2019;432:776–785.
- Gosling J, Jones MI, Arnell A, Watson JE, Venter O, Baquero AC, Burgess ND. A global mapping template for natural and modified habitat across terrestrial earth. *Biol Conserv*. 2020;(250):108974.
- Fagan ME, Kim D-H, Settle W, Ferry L, Drew J, Carlson H, Slaughter J, Schaferbien J, Tyukavina A, Harris NL. The expansion of tree plantations across tropical biomes. *Nat Sustain*. 2022;5:681–688.
- Petersen R, Aksenov D, Goldman E, Sargent S. Mapping tree plantations with multispectral imagery: Preliminary results for seven tropical countries. Technical Note; 2016.
- Poortinga A, Tenneson K, Shapiro A, Nquyen Q, Aung KS, Chishtie F, Saah D. Mapping plantations in Myanmar by fusing Landsat-8, Sentinel-2 and Sentinel-1 data along with systematic error quantification. *Remote Sens*. 2019;11(7):831.
- Didan K. MOD13Q1 MODIS/Terra Vegetation Indices 16-Day L3 Global 250m SIN Grid V006[data set]. *NASA EOSDIS Land Processes DAAC*; 2015; <https://doi.org/10.5067/EOSS/13Q1.006>.
- Mu H, Li X, Wen Y, Huang J, Du P, Su W, Miao S, Geng M. A global record of annual terrestrial human footprint dataset from 2000 to 2018. *Sci Data*. 2022;9:176.
- Danielson JJ, Gesch DB. *Global Multi-resolution Terrain Elevation Data 2010 (GMTED2010)*. Center for Integrated Data Analytics Wisconsin Science Center; 2011.
- ESA. Land Cover CCI Product User Guide Version 2. Tech. Rep. 2017: Available at: maps.elie.ucl.ac.be/CCI/viewer/download/ESACCI-LC-Ph2-PUGv2_2.0.pdf
- Harris N, Goldman ED, Gibbes S. Spatial database of planted trees (SDPT) version 1.0. Technical Note; 2019.
- FAO (Food and Agriculture Organization of the United Nations). *Forest Resources Assessment 2015*. Rome: FAO; 2015.
- Dickmann DI. Silviculture and biology of short-rotation woody crops in temperate regions: Then and now. *Biomass Bioenergy*. 2006;30(8–9):696–705.
- Daugaviete M, Bambi B, Lazdina D, Lazdins A, Makovskis K, Daugavietis U. Plantation forests: A guarantee of sustainable management of abandoned and marginal farmlands. *Chapters*. 2020.
- Schiberna E, Borovics A, Benke A. Economic modelling of poplar short rotation coppice plantations in Hungary. *Forests*. 2021;12(5):623.
- Schulze K, Schepaschenko D, Lesiv M, Fritz S, Verburg PH, Dixon R. Pantropical distribution of short-rotation woody plantations: Spatial probabilities under current and future climate. *Mitig Adapt Strateg Glob Chang*. 2023;28(5):28.
- María P-O, Mercedes T-J, Pedro AG, Javier S-M, César H-M, Fisher score-based feature selection for ordinal classification: A social survey on subjective well-being, in Martínez-Álvarez F, Troncoso A, Quintián H, Corchado E, editors. *Hybrid artificial intelligent systems*. Cham: Springer; 2016.
- Ega B, Df C, Koa D. Evaluation of machine learning algorithms for forest stand species mapping using Sentinel-2 imagery and environmental data in the polish Carpathians. *Remote Sens Environ*. 2020;251:112103.
- Liu L, Gao Y, Zhang X, Chen X. A Dataset of Global Land Cover Validation Samples. 2019; <https://doi.org/10.5281/zenodo.3551995>
- Zhu Z, Woodcock CE. Continuous change detection and classification of land cover using all available Landsat data. *Remote Sens Environ*. 2014;144(1):152–171.
- Cheng Y, Liu H, Wang H, Hao Q. Differentiated climate-driven Holocene biome migration in western and eastern China as mediated by topography. *Earth Sci Rev*. 2018;182:174–185.
- Cánovas-García F, Alonso-Sarría F. Optimal combination of classification algorithms and feature ranking methods for object-based classification of submeter resolution Z/I-imaging DMC imagery. *Remote Sens*. 2015;7(4):4651–4677.

34. Zhang X, Liu L, Chen X, Gao Y, Mi J. GLC_FCS30: Global land-cover product with fine classification system at 30 m using time-series Landsat imagery. *Earth Syst Sci Data*. 2020;13(6):2753–2776.
35. Xu L, Saatchi SS, Yang Y, Yu Y, Pongratz J, Bloom AA, Bowman K, Worden J, Liu J, Yin Y, et al. Changes in global terrestrial live biomass over the 21st century. *Sci Adv*. 2021;7(27):eabe9829.
36. Zhao Y, Gong P, Yu L, Hu L, Li X, Li C, Zhang H, Zheng Y, Wang J, Zhao Y, et al. Towards a common validation sample set for global land-cover mapping. *Int J Remote Sens*. 2013;35(13):4795–4814.
37. Liu L, Gao Y, Zhang X, Chen X. A dataset of European Union land cover validation samples (version v1) [data set]. Zenodo 2020; <https://doi.org/10.5281/zenodo.3998826>
38. Hu Y, Hu Y. Land cover changes and their driving mechanisms in Central Asia from 2001 to 2017 supported by Google earth engine. *Remote Sens*. 2019;11(5):554.
39. Fritz S, See L, Perger C, McCallum I, Schill C, Schepaschenko D, Duerauer M, Karner M, Dresel C, Laso-Bayas JC, et al. A global dataset of crowdsourced land cover and land use reference data. *Sci Data*. 2017;4:170075.
40. Wu X, Jiang X, Liu H, Allen C, Li X, Wang P, Li Z, Yang Y, Zhang S, Shi F, et al. CPDv0: A forest stand structure database for plantation forests in China. *Big Earth Data*. 2022;7(1):212–230.
41. Koskinen J, Leinonen U, Vollrath A, Ortmann A, Lindquist E, Annunzio R, Pekkarinen A, Käyhkö N. Participatory mapping of forest plantations with open Foris and Google Earth Engine. *ISPRS J Photogramm Remote Sens*. 2018;148:63–74.
42. Friedl MA, Sulla-Menashe D, Tan B, Schneider A, Ramankutty N, Sibley A, Huang X. MODIS collection 5 global land cover: Algorithm refinements and characterization of new datasets. *Remote Sens Environ*. 2010;114(1):168–182.
43. Shimada M, Itoh T, Motooka T, Watanabe M, Lucas R, Thapa R, Lucas R. New global forest/non-forest maps from ALOS PALSAR data (2007–2010). *Remote Sens Environ*. 2014;155:13–31.
44. Qin Y, Xiao X, Dong J, Zhang Y, Wu X, Shimabukuro Y, Arai E, Biradar C, Wang J, Zou Z, et al. Improved estimates of forest cover and loss in the Brazilian Amazon in 2000–2017. *Nat Sustain*. 2019;2:764–772.
45. Zhang C, Ju W, Chen JM, Wang X, Yang L, Zheng G. Disturbance-induced reduction of biomass carbon sinks of China's forests in recent years. *Environ Res Lett*. 2015;10(11):114021.
46. Warren C, Sean H, Zhiqiang Y, Stephen S, Brewer C, Evan B, Noel G, Chengqun H, Hughes M, Robert K, et al. How similar are forest disturbance maps derived from different Landsat time series algorithms? *Forests*. 2017;8(4):98.
47. Gong P, Wang J, Yu L, Zhao Y, Lu L, Niu Z, Huang X, Fu H, Liu S, Li C, et al. Finer resolution observation and monitoring of global land cover: First mapping results with Landsat TM and ETM+ data. *Int J Remote Sens*. 2013;34(7):2607–2654.
48. Chen J, Chen J, Liao A, Cao X, Chen L, Chen X, He C, Han G, Peng S, Lu M, et al. Global land cover mapping at 30 m resolution: A POK-based operational approach. *ISPRS J Photogramm Remote Sens*. 2015;103:7–27.
49. Austin KG, Schwantes A, Gu Y, Kasibhatla PS. What causes deforestation in Indonesia? *Environ Res Lett*. 2018;14(2):024007.
50. Hermoso V, Regos A, Morán-Ordóez A. Tree-planting: A double-edged sword to fight climate change in an era of megafires. *Glob Chang Biol*. 2021;27:3001–3003.
51. Leverkus AB, Thorn S, Lindenmayer DB, Pausas JG. Tree planting goals must account for wildfires. *Science*. 2022;376(6593):588–589.
52. Fagan ME, Reid JL, Holland MB, Drew JG, Zahawi RA. How feasible are global forest restoration commitments? *Conserv Lett*. 2020;13(3):e12700.
53. Hansen MC, Potapov PV, Moore H, Turubanova SA, Tyukavina T. High-resolution global maps of 21st-century forest cover change. *Science*. 2013;342(6160):850–853.
54. Adison A, Alejandro M, Paul A, Jaime C, Germán C, Luis C, Taryn FC, Ha A, María JMH, Franco P, et al. Natural forests loss and tree plantations: Large-scale tree cover loss differentiation in a threatened biodiversity hotspot. *Environ Res Lett*. 2020;15(12):124055.
55. Liu L, Zhang X, Gao Y, Chen X, Xie S. Finer-resolution mapping of global land cover: Recent developments, consistency analysis, and prospects. *J Remote Sens*. 2021;2021:5289697.
56. Gu Q, Li Z, Han J. Generalized Fisher score for feature selection. In: *Proceedings of the 27th Conference on Uncertainty in Artificial Intelligence*; 2012. p. 266–273.
57. Pullanagari R, Kereszturi G, Yule I. Integrating airborne hyperspectral, topographic, and soil data for estimating pasture quality using recursive feature elimination with random Forest regression. *Remote Sens*. 2018;10(7):1117.
58. Xu Y, Yu L, Peng D, Zhao J, Gong P. Annual 30-m land use/land cover maps of China for 1980–2015 from the integration of AVHRR, MODIS and Landsat data using the BFAST algorithm. *Sci China Earth Sci*. 2020;63(9):1390–1407.
59. Yang J, Huang X. The 30 m annual land cover dataset and its dynamics in China from 1990 to 2019. *Earth Syst Sci Data*. 2021;13:3907–3925.